Article

Shear Transfer Mechanism between CFRP Grid and EPS Rigid Foam Insulation of Precast Concrete Sandwich Panels

Tugce Sevil Yaman [1,*] and Gregory Lucier [2]

1 Civil Engineering Department, Mersin University, Mersin 33343, Turkey
2 Department of Civil, Construction, and Environmental Engineering, North Carolina State University, Raleigh, NC 27695, USA
* Correspondence: tsevilyaman@mersin.edu.tr; Tel.: +90-324-361-00-01

Abstract: An experimental program was implemented to investigate the shear transfer mechanism of carbon-fiber-reinforced polymer (CFRP) grids and expanded polystyrene (EPS) rigid foam insulation in three wythe precast concrete sandwich wall panels. The purpose of the research was to measure the shear flow capacity and to observe the failure mode(s) of precast concrete sandwich panels manufactured with a CFRP grid shear transfer mechanism between wythes. Six precast concrete sandwich panels were examined by push-out tests in which the center concrete wythe was pushed downward with respect to two outer concrete wythes. It was observed that the average shear flow capacity of the specimens having 2 in (51 mm) thick foam was higher than that of the specimens having 4 in (102 mm) thick foam. In addition, stiffness decreased significantly when the thickness of the EPS insulation increased. The failure mode for the panels included relative displacement between the center concrete wythe and the outer concrete wythes. Test results showed that panels tended to fail by CFRP grid rupture, CFRP grid pull-out, and loss of bond at the concrete/foam interface. Further tests should be performed to fully comprehend the nature of the shear transfer mechanism between the specific CFRP grid used and EPS rigid foam insulation.

Keywords: precast concrete sandwich panel; push-out test; shear transfer mechanism; CFRP grid; EPS rigid foam insulation

1. Introduction

Insulated precast concrete wall panels (sandwich panels) are typically used in building envelope construction. Sandwich wall panels are fabricated generally with two layers of precast concrete separated by an internal rigid insulation layer of selected materials, including expanded polystyrene (EPS), extruded polystyrene (XPS), and rigid polyurethane insulation. The layers, or wythes, of precast concrete are joined together through the foam core using shear connectors, such as traditional wire-truss connectors that are able to provide sufficient shear resistance to achieve a fully-composite or semi-composite behavior. Thermal conductivity of the material used for the shear connectors is a very important consideration, as shear connectors can act as a thermal bridge, allowing undesired heat to pass through the insulation. The concrete wythes can vary in thickness ranging typically from 2 to 6 in (50 to 150 mm). Sandwich wall panels are sometimes designed as load-bearing to support gravity loads, but must always resist lateral loads. Panels of a non-load-bearing style are used to complete a façade without supporting the vertical loads of a building.

Wall panels were introduced in the 1960s as double tees with solid concrete zones joining a fully composite solid concrete topping. Double-tee sandwich panels were strong and structurally efficient, but thermally ineffective. Following double tees, flat sandwich wall panels with solid concrete zones were developed. Later, metal trusses connecting two concrete wythes were used to achieve a better thermal performance; however, metal trusses still caused significant thermal bridges. At the end of the 1980s, non-composite panels were introduced through the use of non-metallic ties to improve thermal performance. These

panels were thermally efficient, but their structural capacity was low since the separated wythes behaved as independent structures in bending. As connector technology improved, those early systems were developed into partially composite panels offering both structural and thermal benefits [1].

Fiber-reinforced polymer (FRP) composites have many advantages for use in pre-stressed precast concrete sandwich wall panel construction. Thermal bridging problems can be overcome by utilizing FRP materials to connect inner and outer concrete wythes, as FRP has a very low thermal conductivity compared to concrete and steel. In addition, the strength-to-weight ratio of FRP is quite high. CFRP in particular has excellent resistance to degradation under fatigue, excellent resistance to corrosion, and is electromagnetically neutral [2].

2. Background

It has been demonstrated by several researchers that precast concrete sandwich panels most typically show a partially composite behavior, especially when designs for wythe transfer other than solid concrete are considered. Tests performed indicate that most methods of wythe connection reliably generate at least a modest degree of shear transfer between concrete wythes [3–5]. Some prominent studies demonstrating the state of the field are summarized below.

Salmon et al. [6] used a new system of truss-shaped glass-fiber-reinforced polymer (GFRP) shear connectors. Test results indicated that usage of GFRP increased thermal performance of panels compared to panels with steel or concrete connecting elements. In addition, a moderate to high level of composite action was obtained.

In 2003, Altus Group produced a fully composite and thermally effective sandwich wall panel by using a carbon-fiber shear connection grid [1]. Frankl et al. [7–9] investigated the behavior of prestressed concrete sandwich panels with a proprietary CFRP grid, C-GRID, as the shear connector. In total, six panels were tested under axial loads and reverse cyclic lateral loads to simulate gravity and wind pressure loads, respectively. Test results indicated that stiffness and degradation of panels were dependent on relative wythe thickness, carbon shear grid amount, and type of rigid foam insulation in the panel cores. It was also observed that panels with expanded polystyrene (EPS) insulation exhibited better strength, deflection, and composite action behaviors than did panels made from extruded polystyrene (XPS) insulations.

Research was undertaken by Bunn [10] to further investigate the proprietary C-GRID CFRP grid/rigid foam insulation system for precast sandwich panels and architectural facades. Their parameters included type and thickness of insulation and spacing between rows of CFRP grids. Experimental findings were utilized to develop an equation to predict shear flow strength of combinations of grid spacing, insulation types, foam thicknesses, and grid orientation. Sopal et al. [11,12] performed similar tests to identify shear transfer mechanism characteristics of the same C-GRID CFRP grid/foam insulation. Parameters included intervals between grids' vertical lines, type of foam, and insulation thickness. Results indicated that an increase in spacing between grid vertical lines provided a rise in shear flow strengths per row of grid, demonstrating the contribution of the insulation-concrete bond. However, an increase in insulation thickness caused a decrease in shear strength. An equation was developed to estimate shear flow strength of the panels, similar to the equation developed by Bunn [10].

Hodicky et al. [13] carried out a research program to investigate the behavior of thin-walled concrete sandwich panels reinforced with basalt fiber reinforced polymer (BFRP) shear connectors. The experimental program consisted of shear tests and flexural tests. Three-dimensional linear elastic analyses were performed. Numerical study results were checked with test results of small- and half-scale panels, and good agreement was observed between the outcomes in the linear elastic range.

Durability and long-term shear transfer between fiber-reinforced polymer and insulation material was evaluated by Kazem et al. [14]. The effect of sustained load and outdoor

exposure on shear strength was examined. Shear strengths of the panels with EPS were greater than those with XPS. It was also discovered that fabrication quality can greatly affect the shear strength. Results indicated that panels made with EPS insulation, a more porous material, were more susceptible to aging compared to XPS panels, a less porous material. However, the results highlighted that a limited period of outdoor exposure did not have a remarkable effect on the ultimate shear strength of the panels with GFRP grid.

A study to analyze different FRP shear connectors for concrete sandwich panels was performed by Woltman et al. [15]. The objective was to reduce thermal bridging while maintaining composite action. The research contained double-shear push-out tests of fourteen specimens. Parameters considered included the FRP connector type, diameter, and end treatment. Test results demonstrated that the adhesion between concrete and foam was rather brittle. Furthermore, it was deduced from the test results that GFRP sand-coated bars had great potential as shear connectors, while bar diameter and end treatment had a relatively trivial effect on the panel strength.

Gara et al. [16] carried out research on sandwich wall panels. Mechanical properties of the internal layers were obtained by shear tests. Eight samples with internal layers of different thicknesses and number of connectors were tested. Test results indicated that the stiffness decreased when the internal layer's thickness increased. In addition, it was observed that the connectors' contribution was negligible compared to the polystyrene's contribution. Later, compression tests with axial and eccentric loads and diagonal compression tests were performed. Additionally, numerical simulations were performed and compared to experimental results.

Choi et al. [17] investigated in-plane shear performance of concrete sandwich panels with and without corrugated shear connectors by push-out tests. The variables comprised the type and thickness of foam and connectors' breadth, pitch, and inside length. Outcomes demonstrated that the type of insulation greatly impacted the bond strength to concrete. In addition, an increase in the width of the connector increased the stiffness and strength. Furthermore, an increase in pitch caused shear strength to increase. A design equation and a database of shear flow values were proposed.

A design tool was developed by Sorensen et al. [18] to predict the behavior of full-scale concrete sandwich wall panels. Push-off test data from 40 small-scale specimens were used. The parameters included wythe thickness, insulation type, and insulation bond. A beam spring model was developed. In addition, parametric work was done to examine the influences of connector strength, pattern, and intensity. It was deduced that a triangular distribution of connectors was more effective.

Jiang et al. [19] completed horizontal direct-shear push-out experiments to investigate the behavior in shear of concrete sandwich panels having steel glass-FRP shear connectors with a W-pattern. Parameters considered included the height, angle, and diameter of the connectors. Researchers performed 12 precast concrete sandwich panel tests reinforced with steel connectors and six panel tests with glass-FRP connectors, glass-FRP pin connecting elements, and truss-type steel connectors. Effects of the different parameters on the shear behavior were analyzed. It was concluded that in order to obtain ductile behavior of the panels, a proper arrangement of connecting element size, spacing, and anchorage locations was compulsory.

Choi et al. [20] investigated the planar behavior in shear of concrete sandwich panels having grid-type GRFP shear connecting elements to provide design properties and equations to determine shear design strength by push-out specimens. Twenty-two specimens were examined in push-out fashion utilizing two different foams, three insulation thicknesses, and two connector grid intervals. Predicted results using the modified ICC-ES equation were utilized to determine the values of toughness index and shear modulus. It was observed that increasing the insulation thickness caused a decrease in the maximum shear flow and the shear modulus.

Nafadi et al. [21] performed six tests to investigate the performance of full-scale prestressed concrete sandwich panels having continuous foam and CFRP shear grids.

Six tests were completed: three with EPS insulation and three with sandblasted XPS insulation. Two million reverse-cyclic horizontal loading cycles were applied to selected panels, corresponding to 45 percent of the lateral load capacity. A constant sustained axial load was included with all tests. The researchers observed that the final behavior of the tested panels was not influenced by prior fatigue loading, as compared to non-cycled reference panels.

3. Scope of the Current Research

In total, six precast concrete sandwich panel specimens were tested in the study. The panels were tested using a typical double-shear 'push-test' specimen with the center concrete wythe of each specimen loaded downward with respect to two outer concrete wythes. Rigid foam insulation was arranged to separate all adjacent wythes, and an experimental CFRP grid was used to create a shear transfer mechanism. The main objective of this research was to investigate the shear transfer mechanism of the CFRP grid in combination with EPS rigid foam insulation.

4. Experimental Program

4.1. General

Six panels were tested in the current study. Each panel comprised three concrete wythes separated by two layers of rigid insulation. Two continuous strips of vertical CFRP grids, oriented to bridge the wythes at 45 degrees, provided the shear transfer mechanism, and one layer of welded wire reinforcement centered in the plane of each concrete wythe provided reinforcement in the plane of each wythe. All panels were 4 ft (1 m) wide by 5 ft (1.5 m) tall. Three identical panels were tested having 2 in (51 mm) thick rigid EPS insulation in a 2-2-4-2-2 configuration. A second set of three identical panels was tested having 4 in (102 mm) rigid EPS insulation in a 2-4-4-4-2 configuration. The six panels tested are outlined in Table 1.

Table 1. Test matrix.

| Specimen Designation	Foam Type	Panel Width [ft]	Grid Spacing [in]	Foam Thickness [in]
EPS.24.2.MMGRID.1				
EPS.24.2.MMGRID.2				2
EPS.24.2.MMGRID.3	EPS	4	24	
EPS.24.4.MMGRID.1				
EPS.24.4.MMGRID.2				4
EPS.24.4.MMGRID.3				

Note: 1 ft = 0.3 m, 1 in = 25 mm.

The three specimens with 2 in (51 mm) thick EPS insulation were constructed with the cross-section shown in Figure 1, and the three specimens with 4 in (102 mm) thick EPS were constructed with the cross-section shown in Figure 2.
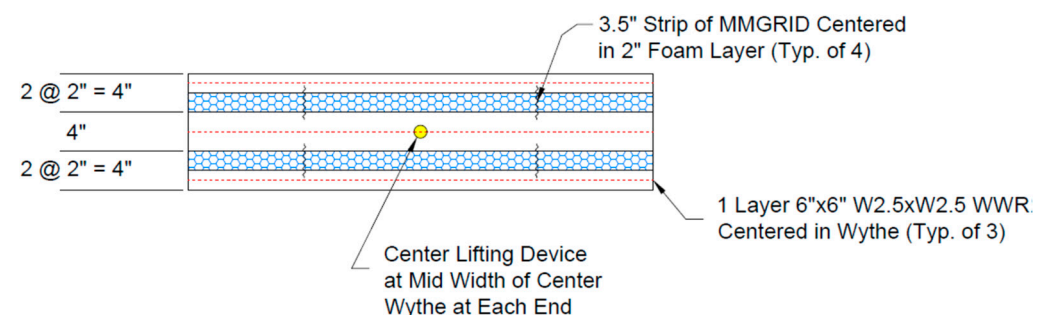

Figure 1. Cross-section of panel specimens with 2.0 in (51 mm) EPS insulation.
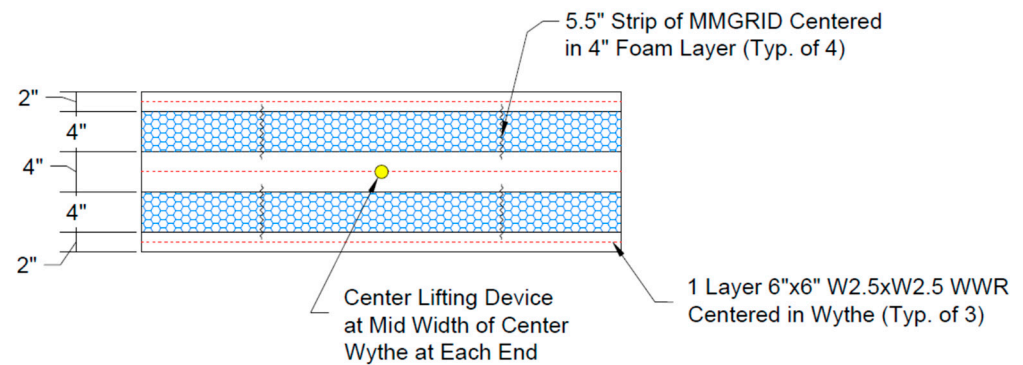
Figure 2. Cross-section of panel specimens with 4 in (102 mm) EPS insulation.

The elevation view common to all specimens is shown in Figure 3. Two continuous strips of vertical CFRP grid were provided between adjacent wythes, and these strips were centered 24 in (610 mm) apart, spaced symmetrically about the panel mid-width.
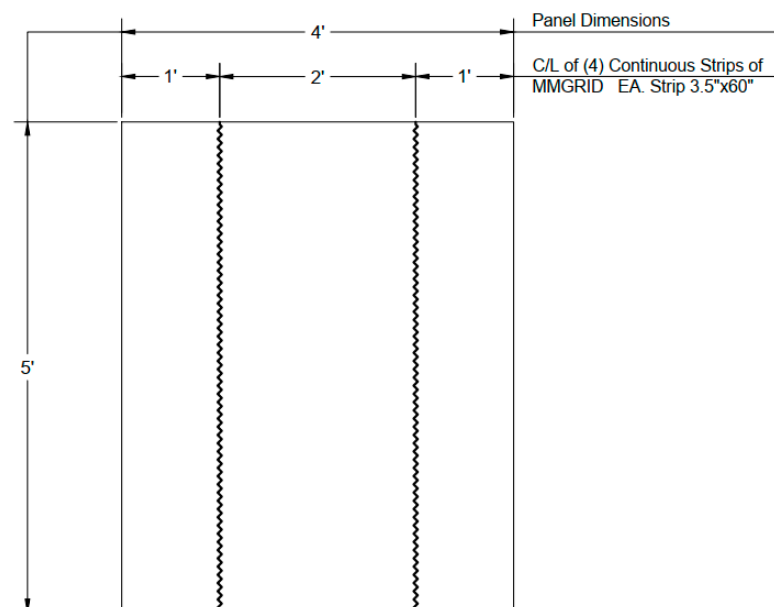
Figure 3. Elevation of all panels showing 24 in (610 mm) spacing between CFRP grid strips.

4.2. Material Properties

The average concrete compressive strength was measured as 6300 psi (43 MPa) at the time of testing. Concrete strength was measured with 4×8 in (102×203 mm) concrete cylinders cast alongside the panel specimens.

The CFRP grid consisted of a 0–90-degree arrangement of warp and weft tows, infused with epoxy resin and linked together at their intersections with small knitting fibers. Grid spacing was a nominal 1 in (25 mm) in each direction. The average strand tensile strength of the CFRP grid specified by Solidian, the manufacturer, is 580 ksi (4000 N/mm^2).

Material properties of the typical EPS insulation are presented in Table 2.

**Table 2.** Material properties of the EPS foam insulation [10].

Foam Type	Density [pcf.]	Compressive Strength (10% Deformation) [psi.]	Modulus of Elasticity [psi.]
EPS	1	10–14	180–220

Note: 1 pcf. = 157 N/m^3, 1 psi. = 6.9 kN/m^2.

4.3. Test Setup

The setup of the push-test experiments is presented in Figure 4. The setup consists of two parallel steel bars, each 2 in (51 mm) wide, placed on the laboratory strong floor. These bars are used to support the outer two concrete wythes, elevating the bottom part of the concrete wythe at the middle off the floor and allowing space for it to displace under load. Loading was exerted to the top of the concrete wythe at the center through a length of 4 in (102 mm) square hollow steel tube (HSS). A 60-ton-capacity hydraulic jack and loadcell were used to apply load to the top surface of the steel tube. The steel tube was centered on the center concrete wythe and was intended to spread the applied load evenly across the panel width.
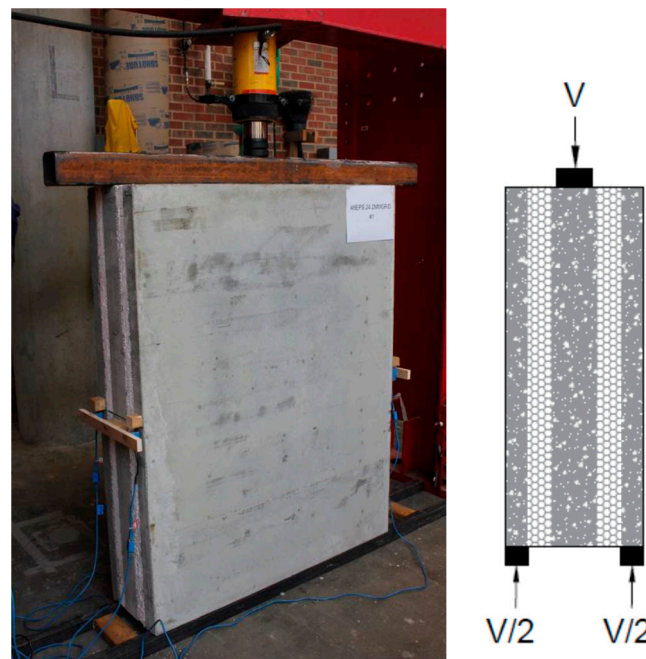

**Figure 4.** Overview of the test setup (**left**) and schematic of the loading (**right**).

4.4. Instrumentation

During each test, the concrete wythe at the middle of a panel was pushed down relative to the two concrete wythes at the sides. The applied load was measured along with the relative vertical deflection between the center and each external concrete wythe at four places around the panel perimeter. All relative deflection measurements were taken at the panel mid-height. All instruments were wired to an electronic data acquisition system. Data were recorded continuously at a sample rate of 1 Hz during loading. Four linear potentiometers measured the relative vertical displacement as shown and labeled in Figure 5. Displacement measurements utilized a support block fixed to the middle wythe and a bar extended from that block over the two exterior wythes. Potentiometers were mounted to each end of the bar. The opposite ends of the potentiometers reacted against blocks fixed to the exterior wythes.

Labels of "front" and "back" correspond to the panel orientation in the laboratory during testing. Labels of "top" and "bottom" correspond to the panel orientation during casting. Thus, location BT (Back Top) corresponds to the potentiometer near the back of the lab on the top wythe (as-cast). In general, the bottom wythe was smooth (steel-form face) and the top wythe was rougher (broom-finished face). Photographs of the panel with potentiometers mounted are presented in Figure 6.
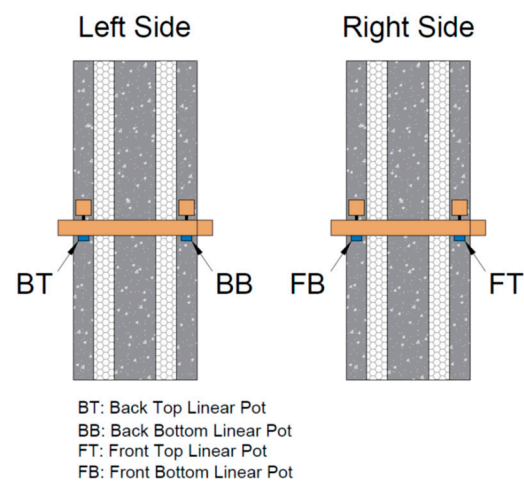
Figure 5. Locations of linear potentiometers for all tests.
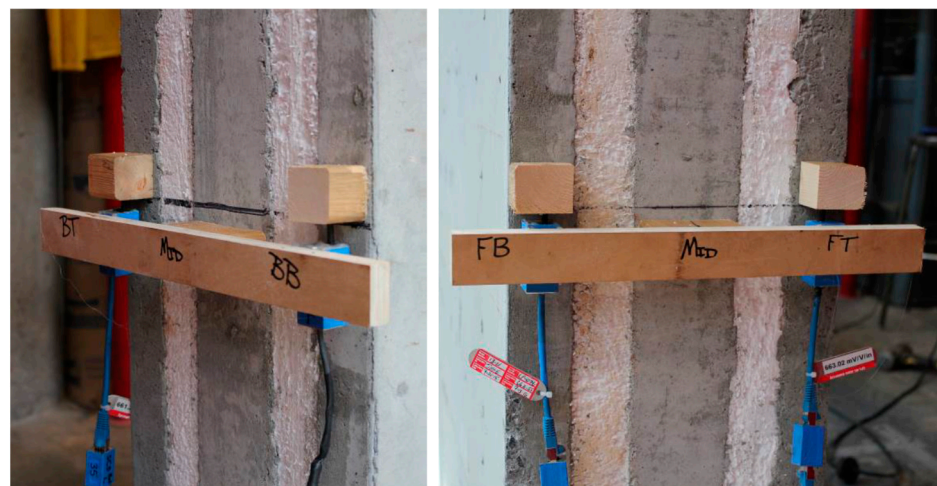
Figure 6. A typical panel with potentiometers installed.

5. Test Results and Discussion

A summary of results is provided in Table 3. The maximum load recorded for each test is presented in the table along with the calculated shear flow. Shear flow was determined as the load carried per grid per unit length of the 60 in (1524 mm) long grid. The peak load per grid was determined as the peak load applied to a specimen divided by the four vertical grids.

Table 3. Summary of results.

Specimen Designation	Peak Load [lbs.]	Shear Flow [lb/in]	Average Shear Flow [lb/in]	Standard Deviation [lb/in]
EPS.24.2.MMGRID.1	74,252	309		
EPS.24.2.MMGRID.2	75,363	314	311	2.7
EPS.24.2.MMGRID.3	74,258	309		
EPS.24.4.MMGRID.1	52,253	218		
EPS.24.4.MMGRID.2	58,924	246	225	18.5
EPS.24.4.MMGRID.3	50,531	211		

Note: 1 lb = 4.5 N, 1 lb/in = 0.2 N/mm.

The results indicate the average shear flow capacity of the panels having 2 in (51 mm) thick insulation was higher than that of panels having 4 in (102 mm) thick insulation. The average shear flow achieved prior to failure was 311 lb/in (54.5 N/mm) for 2 in (51 mm) thick foam insulation and 225 lb/in (39 N/mm) for 4 in (102 mm) thick foam insulation.

5.1. Specimens with 2″ Insulation

The panels with 2″ insulation are shown after testing in Figure 7. Substantial slip between the concrete wythes can be observed in all cases after failure, including obvious shear through the rigid insulation in the cases of panels 1 and 3. Individual sensor measurements for each panel are plotted vs. the applied load in Figures 8–10.

Figure 7. Panels EPS.24.2.MMGRID.1 (**left**), 2 (**middle**), and 3 (**right**) after testing.
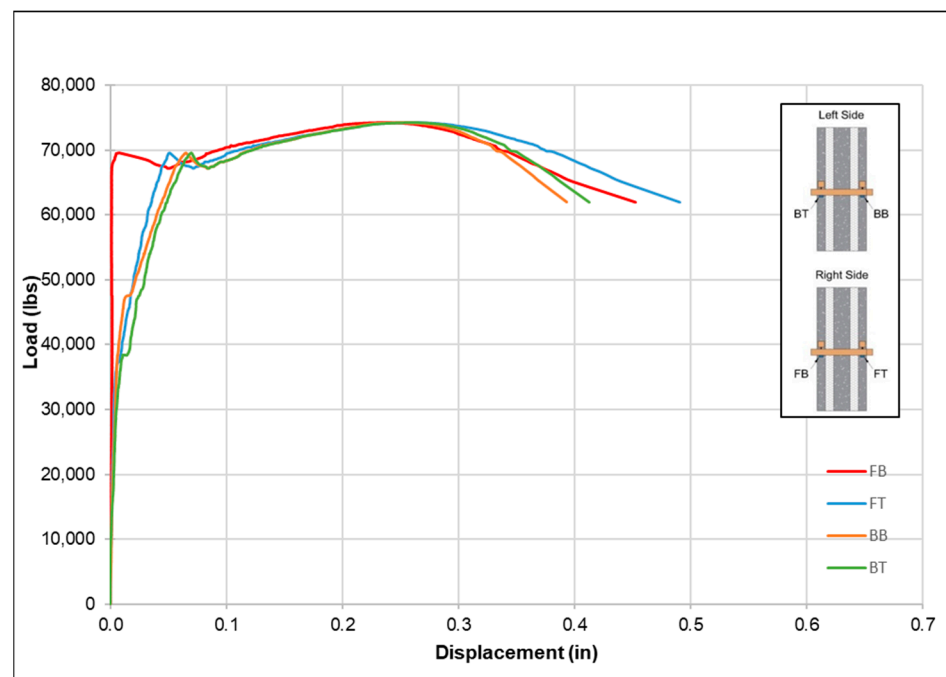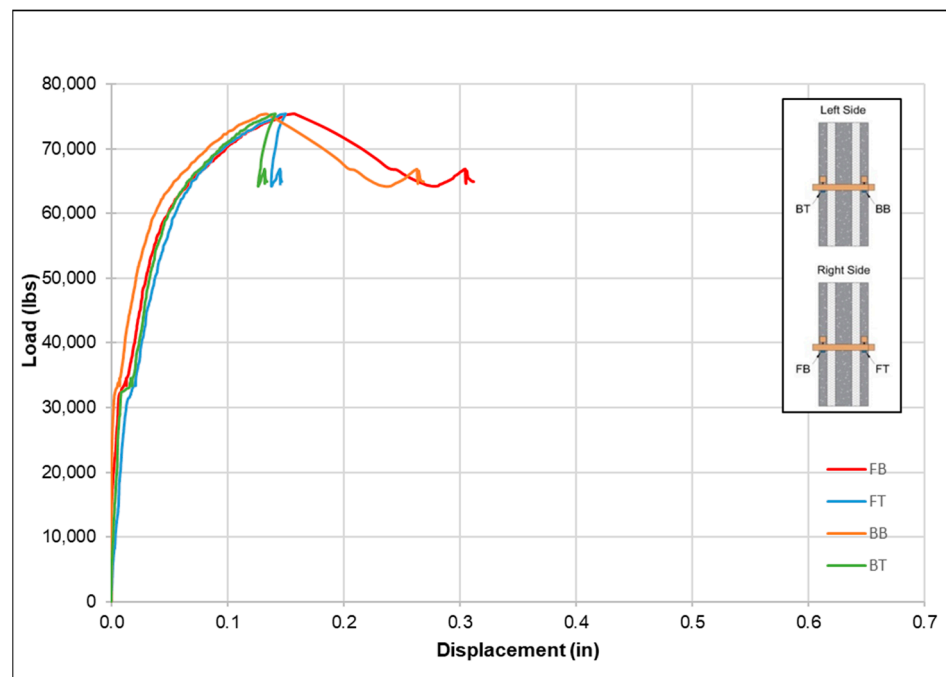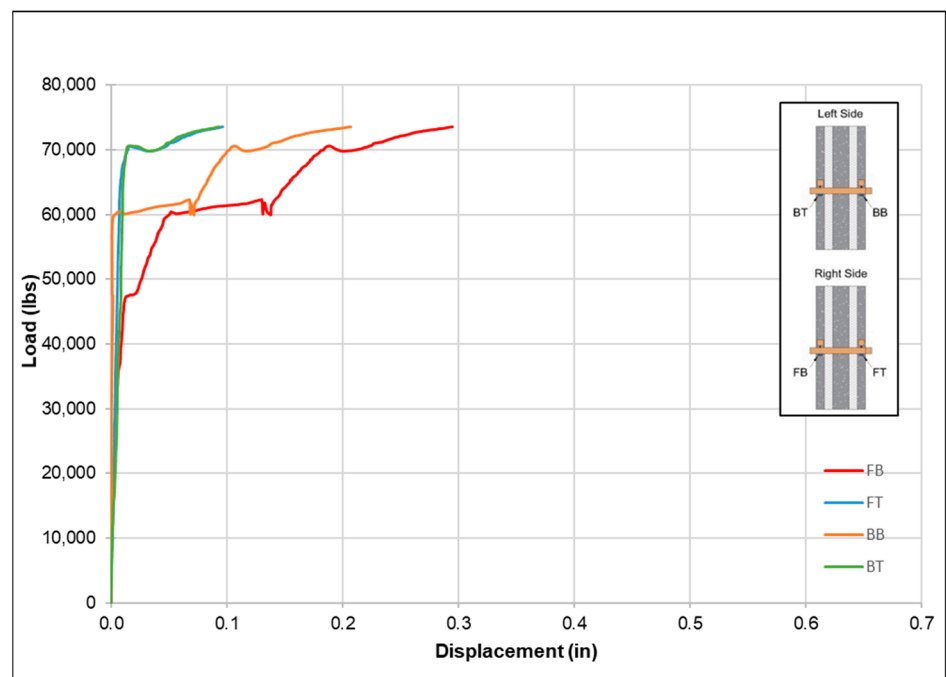

Figure 8. Load vs. displacement data from the four sensors for EPS.24.2.MMGRID.1.

Figure 9. Load vs. displacement data from the four sensors for EPS.24.2.MMGRID.2.

Figure 10. Load vs. displacement data from the four sensors for EPS.24.2.MMGRID.3.

5.2. Specimens with 4″ Insulation

The panels with 4″ insulation are shown after testing in Figure 11. Slip and separation at the concrete-insulation interface is observed at failure, with no signs of shear cracking in the insulation itself. Individual sensor measurements for this panel are plotted vs. the applied load in Figures 12–14.

Figure 11. Panels EPS.24.4.MMGRID.1 (**top**), 2 (**middle**), and 3 (**bottom**) after testing.

5.3. Comparison of the EPS.24.2.MMGRID Specimens with 2″ Insulation

Load vs. average relative displacement graphs of specimens with 2 in (51 mm) EPS insulation are presented in Figure 15. It is noted that, while load-deflection behaviors are shown, the general shape of the behavior can also be thought of as reflective of the average shear stress–shear strain behavior of the panels. Specimens showed similar load carrying capacities, but somewhat different load-deformation responses, especially in the highly non-linear regions of the response. Load-displacement behaviors largely aligned through the elastic portion of the behavior through approximately 30,000 lbs (133 kN) of applied load. The observed modest variations in shear strength and late stage deformations can be attributed to minor expected differences in manufacturing from panel to panel.
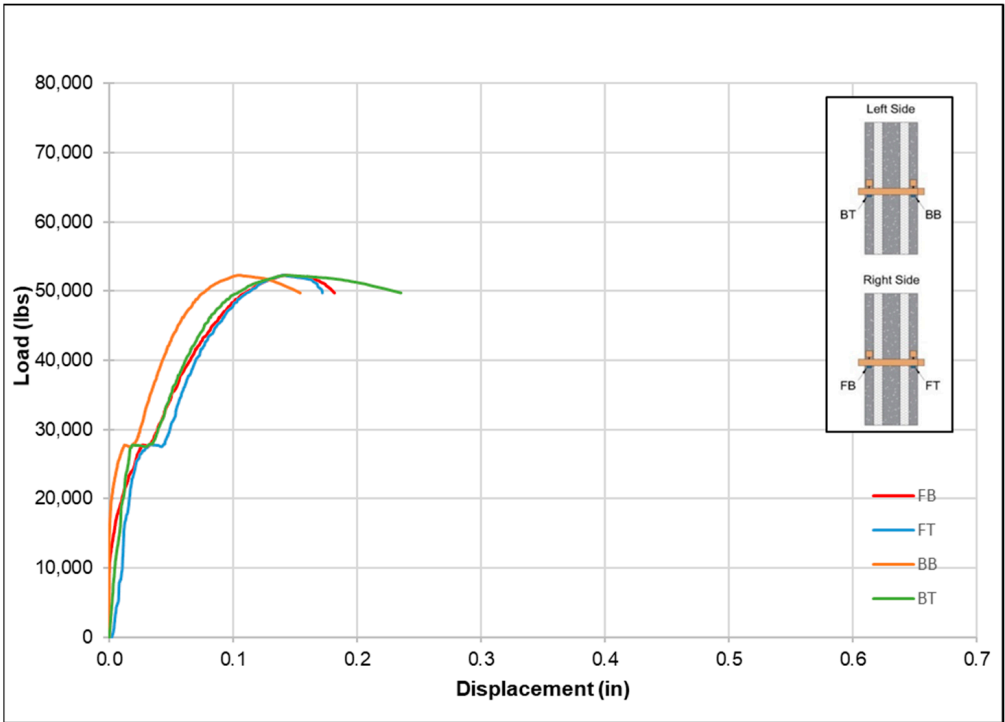
Figure 12. Load vs. displacement data from the four sensors for EPS.24.4.MMGRID.1.
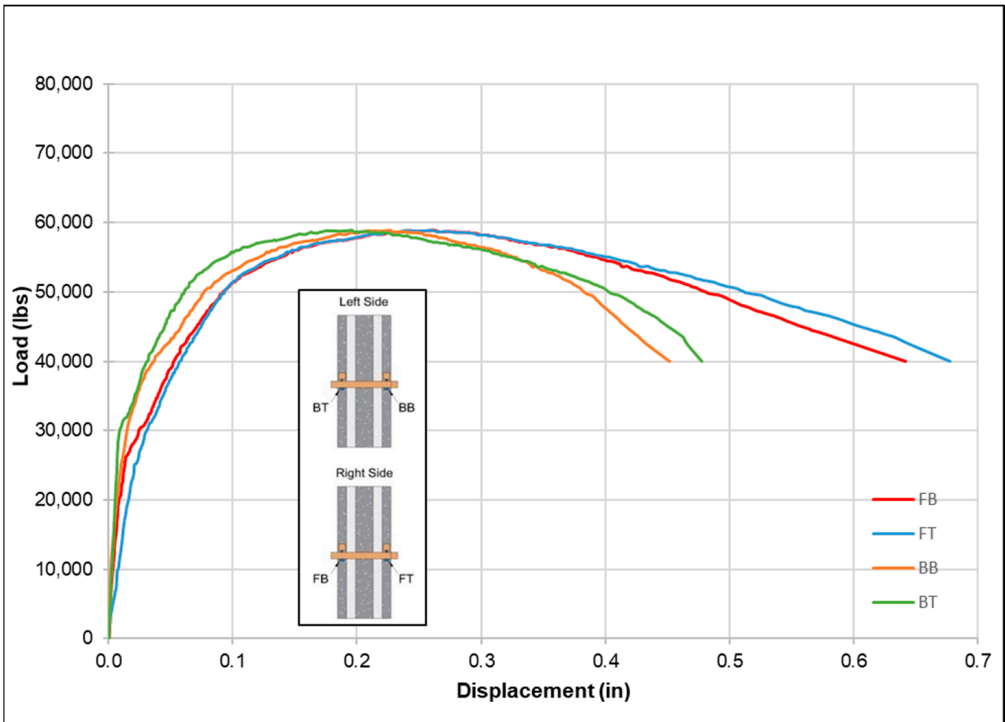

Figure 13. Load vs. displacement data from the four sensors for EPS.24.4.MMGRID.2.
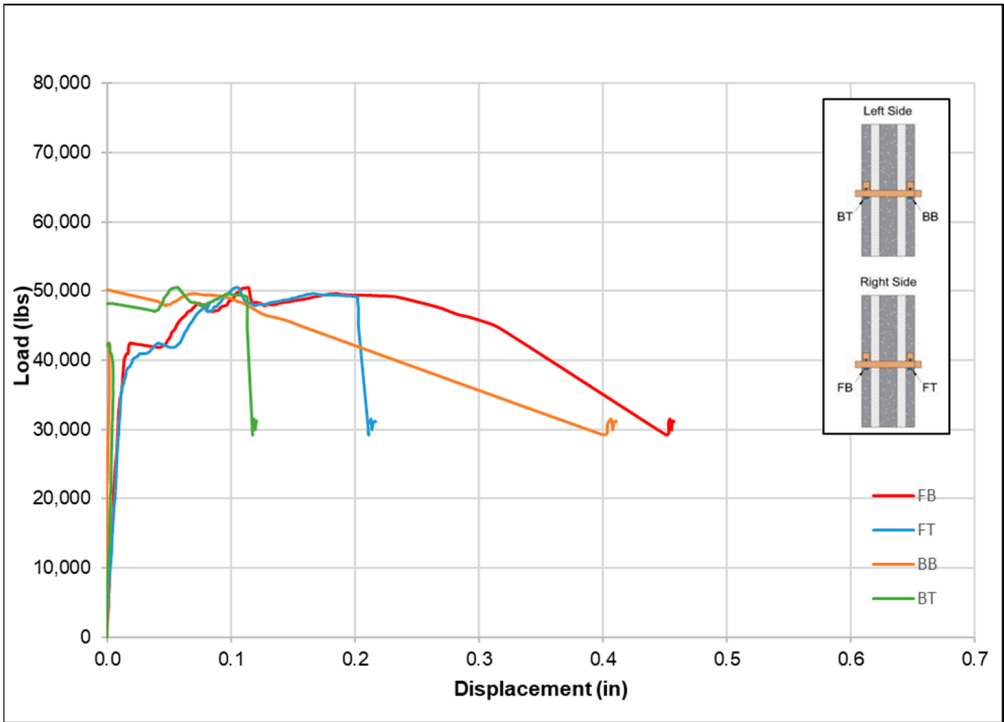
Figure 14. Load vs. displacement data from the four sensors for EPS.24.4.MMGRID.3.
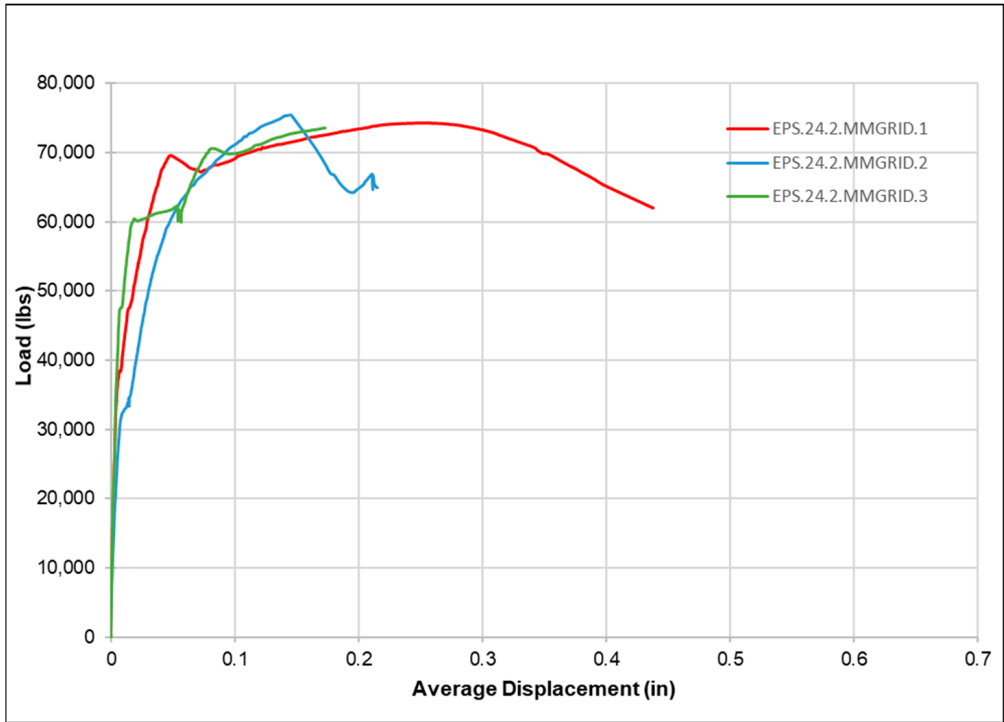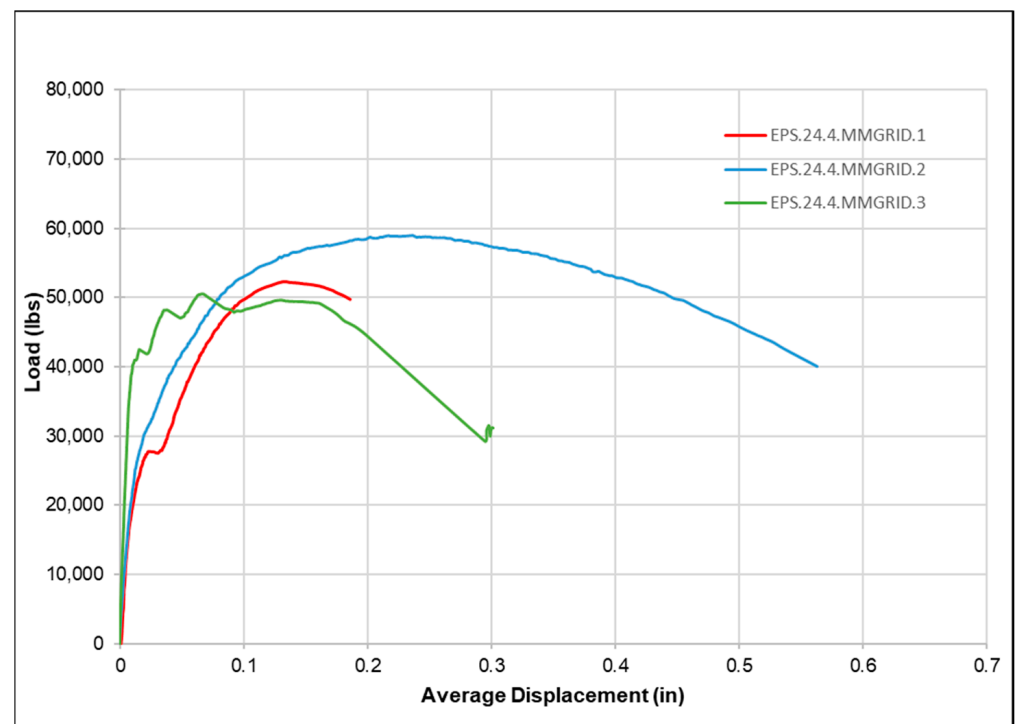

Figure 15. Average displacement behavior for each of the three specimens having 2 in (51 mm) EPS.

5.4. Comparison of EPS.24.4.MMGRID Specimens with 4″ Insulation

The average load-displacement response of the EPS.24.4.MMGRID specimens is presented in Figure 16. For the 4 in (102 mm) thick insulation, differences in load-carrying capacity and in deformations in the non-linear ranges of response are more pronounced across the set of three panels. Shear strain of the CFRP grid will be higher in panels with the thicker insulation (for a given applied load), which likely accounts for some of the additional variability. A linear elastic limit of approximately 20,000 lbs. (89 kN) is observed.


Figure 16. Average displacement behavior for each of the three specimens having 4 in (102 mm) EPS.

5.5. Effect of Rigid Foam Insulation Thickness

Influence of the EPS foam insulation's thickness was investigated by comparing the shear flow vs. average deflection graphs of all EPS.24.2.MMGRID to all EPS.24.4.MMGRID specimens, as demonstrated in Figure 17. Increasing the thickness of the EPS insulation from 2 in (51 mm) to 4 in (102 mm) decreased both the shear flow capacity and the linear-elastic limit of the load-deflection behavior by about 30%. Stiffness of the inter-wythe mechanism also decreased considerably with increased insulation thickness in both the elastic and non-linear regions. The displacement required to reach peak load was roughly similar for each group of panels, despite the much lower peak load for panels with thicker insulation.

5.6. Failure Modes

The observed failure mode for all panels included relative displacement of the center concrete wythe relative to the outer concrete wythes, as shown for a selected panel in Figure 18. The panel specimens failed by a combination of CFRP grid rupture, CFRP grid pull-out, degradation of the EPS insulation in shear, and loss of concrete–foam bond, as illustrated in Figure 19. All panels exhibited rupture of some strands of the internal CFRP grid, as evidenced by audible cracking sounds observed during all tests, and confirmed by subsequent inspection post-test. All panels also appeared to exhibit at least some grid failure due to pull-out from the concrete, as evidenced by post-test inspections shown in Figures 20 and 21.
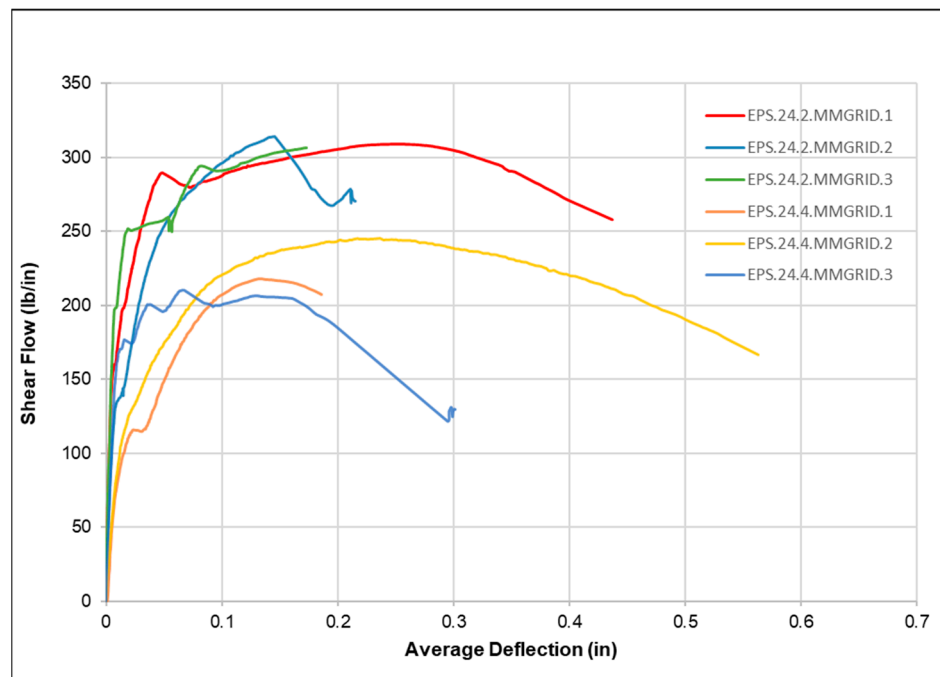
Figure 17. Effect of EPS insulation thickness: shear flow vs. average deflection graph of EPS.24.2.MMGRID and EPS.24.4.MMGRID specimens.


Figure 18. View of a typical failure mode showing shear between wythes.

The observed failure modes and behaviors are consistent with those observed in the literature by various researchers. Bunn [10] found that, as the thickness of the EPS insulation foam increases, the shear flow strength decreases, which was observed in the current study. Likewise, Sopal et al. [11,12] observed that an increase in foam thickness resulted in a decrease in shear strength. Woltman et al. [15] showed that the adhesion between concrete and foam was quite brittle, as was illustrated here in Figures 19 and 20. Gara et al. [16] concluded that stiffness decreased when the internal layer's thickness increased. Choi et al. [20] found that increasing the insulation wythe thickness caused a decrease in the maximum shear flow and the shear modulus. Decreasing shear stiffness relative to increasing insulation thickness was observed in the current specimens, confirming the prior studies. These results together indicate that the experimental CFRP grid utilized in the current work exhibits generally similar behavior to other grid systems tested in the literature.

Figure 19. A failure showing substantial deformation in the foam prior to loss of bond.
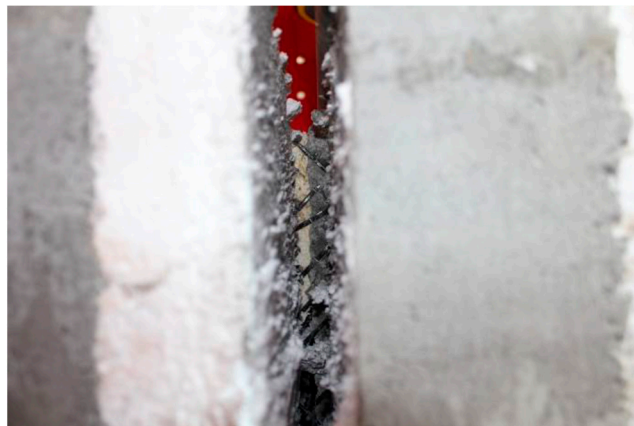
Figure 20. Typical view of combined rupture and pull-out failure mode.

Figure 21. View of ruptured and pulled-out grid.

6. Analysis

The purpose of the test program was to examine the shear transfer mechanism of a new type of CFRP grid used as a shear transfer mechanism with EPS rigid foam insulation in concrete sandwich wall panels. The shear modulus G was determined in accordance with the International Code Council Evaluation Service (ICC-ES) Acceptance Criteria-Semi-Continuous Fiber-Reinforced Grid Connectors Used in Combination with Rigid Insulation in Concrete Sandwich Panel Construction (AC422) [22] equation. In addition, a design equation developed by Bunn [10] for another type of CFRP grid was employed to compare the shear flow capacity of the currently tested CFRP grid and rigid foam insulation to prior results in the literature. The equation proposed in the ICC-ES AC422 [22] based on a 99.7% confidence interval was also utilized to find the nominal shear design strength. In addition, the modified ICC-ES AC422 [22] equation proposed by Choi et al. [17] utilizing an 80% confidence interval was evaluated.
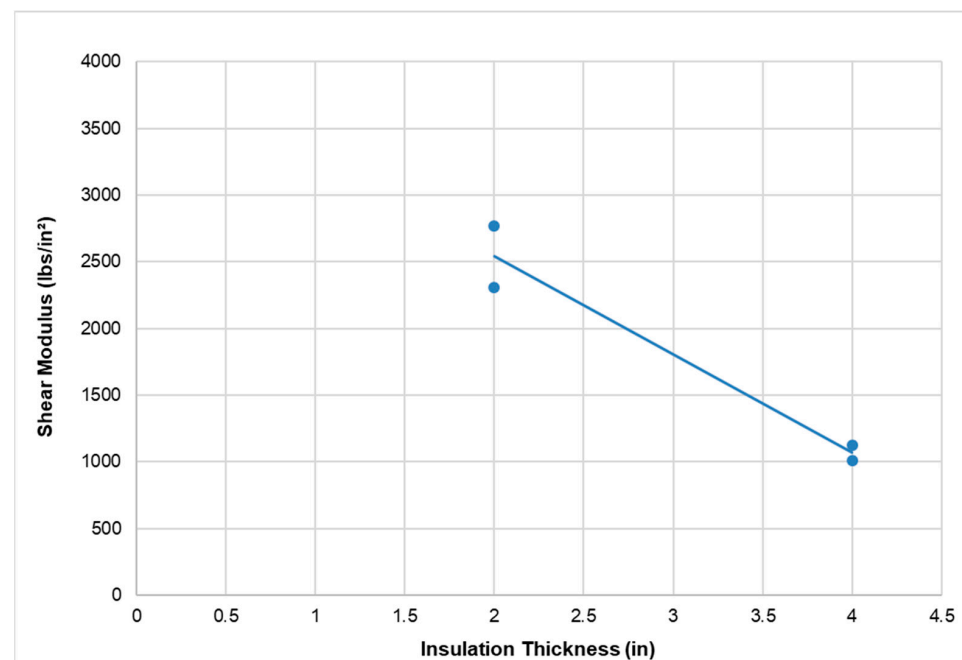
6.1. Shear Modulus

The shear modulus can be calculated by utilizing push-out test specimens' deformation values according to the ICC-ES AC422 [22] equation given in Equation (1) [22].

$$G_i = \frac{0.5V_{i,max}}{A_{sa}} \cdot \frac{t}{\Delta_{i,v}} = \frac{0.5V_{i,max}}{2Lw} \cdot \frac{t}{\Delta_{i,v}} \tag{1}$$

where $V_{i,max}$ is the peak load level of the specimen (kN), G_i is the shear modulus of the specimen (kN/mm^2), t is the thickness of the rigid foam (mm), L is the length of the grid segment and specimen (mm), A_{sa} is the total contact surface area between the insulation and both surfaces of the central concrete wythe (mm^2), w is the width of the specimen (mm), and $\Delta_{i,v}$ is the relative displacement between the central concrete core and the two outer concrete wythes of the specimen at 50% of the peak load level (mm).

The shear modulus values determined by Equation (1) [22] versus insulation thickness graph is presented in Figure 22. A scattering value in each insulation thickness set, which can be attributed to minor differences in manufacturing, was discarded. The shear modulus values were observed to decrease when the thickness of the EPS insulation increased.

Figure 22. Shear modulus vs. insulation thickness graph of EPS.24.2.MMGRID and EPS.24.4.MMGRID specimens.

6.2. Design Equation

The nominal shear flow capacity of the CFRP grid and EPS insulation system tested by Bunn [10] is predicted by Equation (2). This equation modifies a baseline shear flow capacity with constants developed for various foam types, thickness, grid spacing, and grid orientation. This method enables the prediction of shear flow capacity given a set of selected parameters. Notably, this equation was developed and calibrated to 66 tests of a different CFRP grid system than that tested here [10].

$$q_n = \gamma_{type} * \gamma_{thickness} * \gamma_{spacing} * \gamma_{orientation} * q_{baseline} \tag{2}$$

The equation parameters include: q_n the nominal shear flow capacity of the grid (lb/in), γ_{type} gamma factor for insulation type, $\gamma_{thickness}$ gamma factor for insulation thickness, $\gamma_{spacing}$ gamma factor for grid spacing, $\gamma_{orientation}$ gamma factor for grid orientation (vertical or transverse), and $q_{baseline}$ baseline shear flow capacity of grid (lb/in). The gamma factors and baseline recommended by Bunn [10] are presented in Table 4.

Table 4. Gamma factors determined by Bunn [10].

EPS	γ_{type}	Insulation Thickness [in]	$\gamma_{thickness}$	Grid Spacing [in]	$\gamma_{Spacing}$	Orientation	$\gamma_{orientation}$	$q_{baseline}$ [lb/in]
	1.8	2	1.5	24	1.2	Vertical	1	100
		4	1.3					

Note: 1 in = 25 mm, 1 lb/in = 0.2 N/mm.

The only standardized approach currently available for testing precast concrete wall panels with continuous grid wythe connections is the ICC-ES AC422 [22]. The acceptance criteria examine the results of multi-wythe push tests by calculating the measured shear flow for each test specimen in the same manner as was presented above. Shear flow is defined by the ICC-ES AC422 [22] as the maximum load sustained in a given push test divided by the total length of grid resisting that applied force.

The nominal shear design strength was determined by the Equation (3) of the ICC-ES AC422 [22], which arrives at design values for shear flow by subtracting three standard deviations from the mean result for a given set of tests [22].

$$q_n = q_{a,max} - 3\sigma_p \tag{3}$$

where q_n is the nominal shear flow in kN/mm, $q_{a,max}$ is the mean shear flow in kN/mm, and σ_p is the standard deviation of the peak test loads of the specimens. Choi et al. [17] modified the ICC-ES AC422 [22] equation, Equation (4), utilizing an 80% confidence interval to increase the efficiency of the shear connectors [17].

$$q_n = q_{a,max} - 1.3\sigma_p \tag{4}$$

q_n being the nominal shear flow in kN/mm, $q_{a,max}$ the mean shear flow in kN/mm, and σ_p the standard deviation of the peak test loads of the specimens.

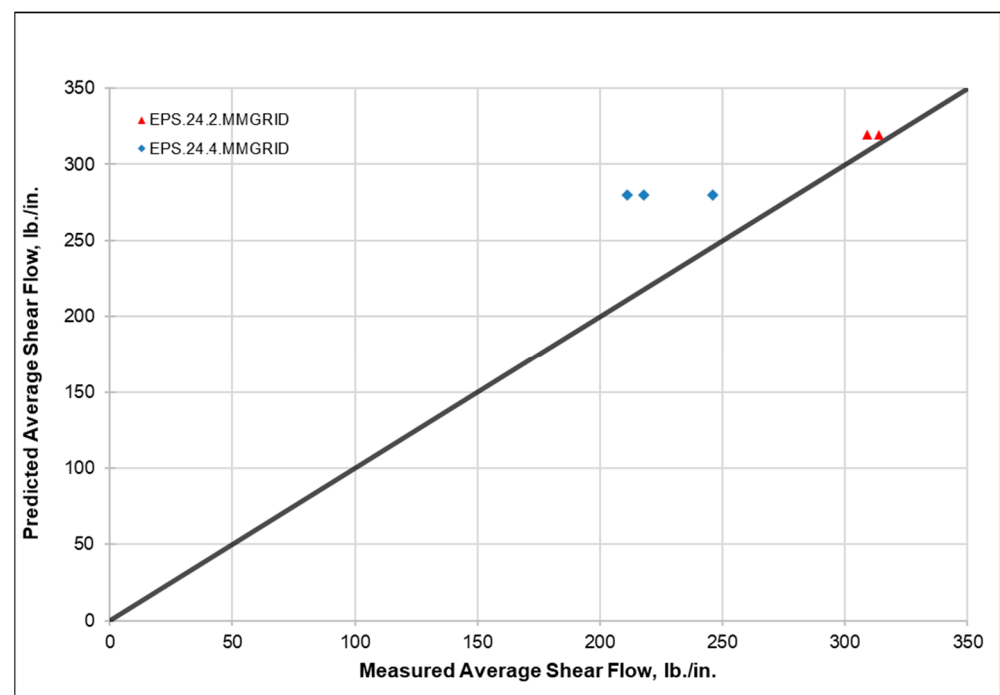### 6.3. Predicted vs. Measured Average Shear Flow Capacities

The predicted values determined by the design equation [10] are compared with the measured values from the current tests in Table 5. Moreover, test results are compared with the predicted values graphically in Figure 23. It can be observed from the figure that the predicted and the measured values match each other better for 2 in (51 mm) insulation thickness than for 4 in (102 mm) insulation. In general, for a prediction to be conservative, all points should fall below the line shown in Figure 23. While the difference between predicated shear flow and average shear flow is within 5% for the 2″ (51 mm)

insulation, all measured values fall on the non-conservative side of the prediction. For 4″ (102 mm) insulation, the prediction is nearly 25% high, indicating a significant overestimation of capacity. These results clearly indicate that the CFRP grid system tested by Bunn [10] developed higher shear flow capacities than did the CFRP grid system tested here, even though the systems were nominally similar. This finding demonstrates the importance of having system-specific test data for a given sandwich panel wythe shear transfer mechanism.

**Table 5.** Comparison of measured and estimated mean shear flow capacities.

| Specimen Designation	Insulation Type	Insulation Thickness [in]	Grid Spacing [in]	Measured Shear Flow Capacity [lb/in]	Predicted Shear Flow Capacity [lb/in]
EPS.24.2.MMGRID.1				309	
EPS.24.2.MMGRID.2		2		314	324
EPS.24.2.MMGRID.3	EPS		24	309	
EPS.24.4.MMGRID.1				218	
EPS.24.4.MMGRID.2		4		246	281
EPS.24.4.MMGRID.3				211	

Note: 1 in = 25 mm, 1 lb/in = 0.2 N/mm.

Figure 23. Predicted values from the design equation [10] vs. measured average shear flow (1 lb/in = 0.2 N/mm).

The predicted values according to Equation (3) [22] and Equation (4) [17] are compared with the measured values in Figures 24 and 25, respectively. It was observed that more conservative results were obtained by Equation (4) [17] than Equation (3) [22]. These shear flow design values are specific to the particular carbon grid system tested, including the spacing of that grid as used in the test specimens, and the type of insulation used in the tests.
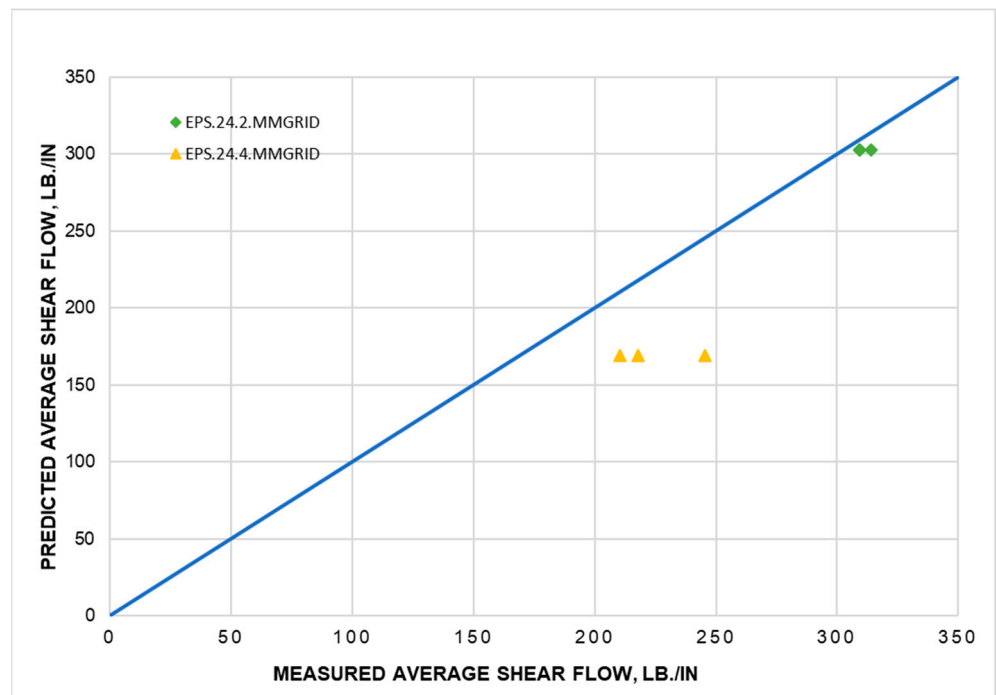
Figure 24. Predicted values from the ICC-ES AC422 equation [22] based on a 99.7% confidence interval vs. measured average shear flow (1 lb/in = 0.2 N/mm).
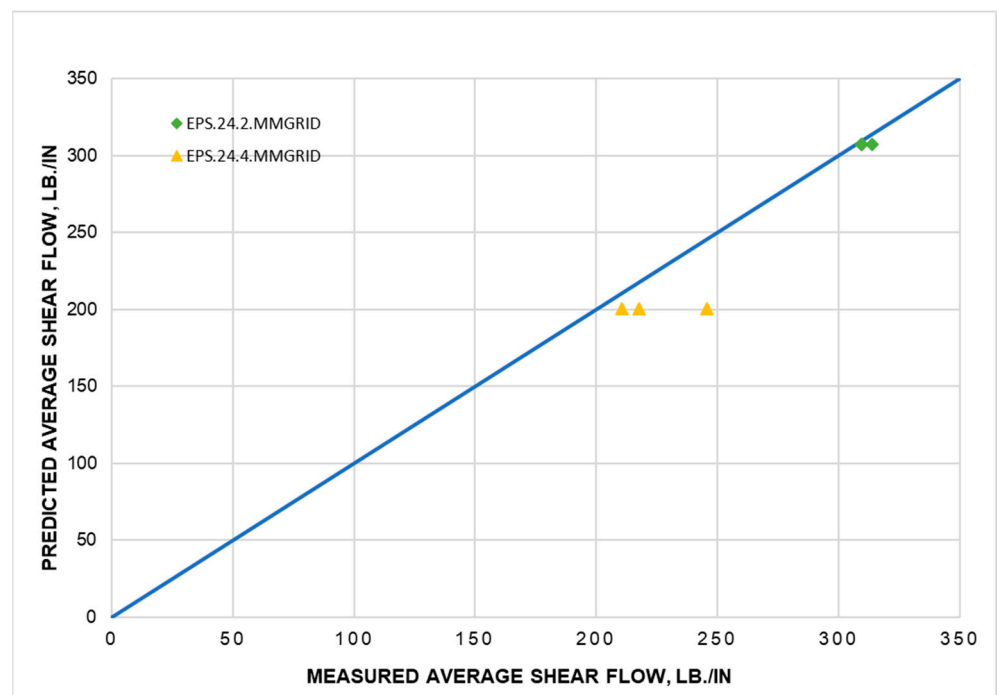
Figure 25. Predicted values from the Choi et al. equation [17] based on a 80% confidence interval vs. measured average shear flow (1 lb/in = 0.2 N/mm).

7. Conclusions

In summary, this research presented double-shear push tests of six precast concrete sandwich panel specimens. Tests were performed to failure to determine shear flow capacity of each panel. An experimental CFRP grid system was used to transfer shear between the concrete wythes, and results were compared to predications available in the literature for

a similar CFRP grid wythe connection system. Two different insulation thicknesses were tested, with three identical tests of each condition conducted. Results indicated that panels with 2 in (51 mm) thick insulation had higher shear strengths compared to the specimens having 4 in (102 mm) thick insulation, a finding confirmed by many sources in the literature. The current tests demonstrated an approximately 30% drop in shear flow capacity when increasing insulation thickness to 4 in (102 mm) from 2 in (51 mm).

Likewise, the results also indicate that the elastic stiffness and the post-elastic stiffness of the load-deflection behaviors both reduce with increasing insulation thickness. Doubling the insulation thickness resulted in an approximate 30% drop in stiffness across the range of behavior. In addition, the variability of the test results in increased deformation with increasing insulation thickness, likely due to the higher shear strain demands placed on the CFRP grids. Failure of all panels included a combination of CFRP grid rupture, CFRP grid pull-out, and loss of concrete/foam bond. The rigid insulating foam was more likely to shear in specimens with thinner insulation.

Critically, the current test results demonstrate that design methods developed for similar CFRP grid shear transfer systems do not directly apply to the tested system, despite the nominal similarities. Published prediction methods calibrated to test results of other CFRP grid and EPS insulation systems overestimated performance of the current system by as much as 25%. Given this finding, designers must be careful to apply only system-specific test data to a sandwich wall panel wythe transfer mechanism. As such, a much larger suite of tests would be required to fully qualify the performance of the tested CFRP grid system before field implementation.

Author Contributions: Conceptualization, T.S.Y. and G.L.; methodology, T.S.Y. and G.L.; validation, T.S.Y.; formal analysis, T.S.Y.; investigation, T.S.Y. and G.L.; resources, T.S.Y. and G.L.; data curation, T.S.Y.; writing—original draft preparation, T.S.Y.; writing—review and editing, T.S.Y. and G.L.; visualization, T.S.Y.; supervision, G.L.; project administration, G.L.; funding acquisition, G.L. All authors have read and agreed to the published version of the manuscript.

Data Availability Statement: The data presented in this study are available on request from the corresponding author.

Conflicts of Interest: The authors declare no potential conflict of interest with respect to the research, authorship, and/or publication of this article.

References

1. Gleich, H. New carbon fiber reinforcement advances sandwich wall panels. *Structure Magazine*, April 2007; pp. 61–63.
2. Erki, M.A.; Rizkalla, S.H. FRP reinforcement for concrete structures. *Concr. Int.* **1993**, *15*, 48–53.
3. Pessiki, S.; Mlynarczyk, A. Experimental evaluation of composite behavior of precast concrete sandwich wall panels. *PCI J.* **2003**, *48*, 54–71. [CrossRef]
4. Lee, B.; Pessiki, S. Design and analysis of precast, prestressed concrete three-wythe sandwich wall panels. *PCI J.* **2007**, *52*, 70–83. [CrossRef]
5. Bush, T.D.; Stine, G.L. Flexural behavior of composite prestressed sandwich panels. *PCI J.* **1994**, *39*, 112–121. [CrossRef]
6. Salmon, D.C.; Einea, A.; Tadros, M.K.; Culp, T.D. Full scale testing of precast concrete sandwich panels. *ACI Struct. J.* **1997**, *94*, 354–362.
7. Frankl, B. Structural Behavior of Insulated Precast Prestressed Concrete Sandwich Panels Reinforced with CFRP Grid. Master's Thesis, North Carolina State University, Raleigh, NC, USA, 2008.

8. Frankl, B.; Lucier, G.; Rizkalla, S.; Blaszak, G.; Harmon, T. Structural behavior of insulated prestressed concrete sandwich panels reinforced with FRP grid. In Proceedings of the Fourth International Conference on FRP Composites in Civil Engineering (CICE2008), Zurich, Switzerland, 22–24 July 2008.

9. Frankl, B.A.; Lucier, G.W.; Hassan, T.K.; Rizkalla, S.H. Behavior of precast, prestressed concrete sandwich wall panels reinforced with CFRP shear grid. *PCI J.* **2011**, *56*, 42–54. [CrossRef]

10. Bunn, W.G. CFRP Grid/Rigid Foam Shear Transfer Mechanism for Precast, Prestressed Concrete Sandwich Wall Panels. Master's Thesis, North Carolina State University, Raleigh, NC, USA, 2011.

11. Sopal, G.J. Use of CFRP Grid as Shear Transfer Mechanism for Precast Concrete Sandwich Wall Panels. Ph.D. Thesis, North Carolina State University, Raleigh, NC, USA, 2013.

12. Hodicky, K.; Sopal, G.; Rizkalla, S.; Hulin, T.; Stang, H. Experimental and numerical investigation of the FRP shear mechanism for concrete sandwich panels. *ASCE J. Compos. Constr.* **2015**, *19*, 1–12. [CrossRef]

13. Hodicky, K.; Hulin, T.; Schmidt, J.W.; Stang, H. Structural performance of new thin-walled concrete sandwich panel system reinforced with BFRP shear connectors. In Proceedings of the Fourth Asia-Pacific Conference on FRP in Structures, Melbourne, Australia, 11–13 December 2013.

14. Kazem, H.; Bunn, W.G.; Seliem, H.M.; Rizkalla, S.H.; Gleich, H. Durability and long term behavior of FRP/foam shear transfer mechanism for concrete sandwich panels. *Constr. Build. Mater.* **2015**, *98*, 722–734. [CrossRef]

15. Woltman, G.D.; Tomlinson, D.G.; Fam, A. A comparative study of various FRP shear connectors for sandwich concrete walls. In Proceedings of the CICE 2010—The 5th International Conference on FRP Composites in Civil Engineering, Beijing, China, 27–29 September 2010.

16. Gara, F.; Ragni, L.; Roia, D.; Dezi, L. Experimental tests and numerical modelling of wall sandwich panels. *Eng. Struct.* **2012**, *37*, 193–204. [CrossRef]

17. Choi, K.-B.; Choi, W.-C.; Feo, L.; Jang, S.-J.; Yun, H.-D. In-plane shear behavior of insulated precast concrete sandwich walls reinforced with corrugated GFRP shear connectors. *Compos. Part B* **2015**, *79*, 419–429. [CrossRef]

18. Sorensen, T.; Olsen, J.; Maguire, M. *Shear Testing of Precast Concrete Sandwich Wall Panel Composite Shear Connectors*; Civil and Environmental Engineering Department, Utah State University: Logan, UT, USA, 2016.

19. Jiang, H.; Guo, Z.; Liu, J.; Liu, H. The shear behavior of precast concrete sandwich panels with W-shaped SGFRP shear connectors. *KSCE J. Civ. Eng.* **2018**, *22*, 3961–3971. [CrossRef]

20. Choi, W.; Jang, S.-J.; Yun, H.-D. Design properties of insulated precast concrete sandwich panels with composite shear connectors. *Compos. Part B Eng.* **2019**, *157*, 36–42. [CrossRef]

21. Nafadi, M.K.; Lucier, G.; Sevil Yaman, T.; Gleich, H.; Rizkalla, S. Long-term behavior of precast, prestressed concrete sandwich panels reinforced with carbon-fiber-reinforced polymer shear grid. *PCI J.* **2021**, *66*, 23–38. [CrossRef]

22. ICC. *AC422 Semicontinuous Fiber-Reinforced Grid Connectors Used in Combination with Rigid Insulation in Concrete Sandwich Panel Construction*; ICC-ES: Brea, CA, USA, 2022.